Does spatial configuration matter? Understanding the effects of land cover pattern on land surface temperature in urban...

Article *in* Landscape and Urban Planning · July 2011

DOI: 10.1016/j.landurbplan.2011.03.009

3 authors:

Weiqi Zhou
Chinese Academy of Sciences

Ganlin Huang
Beijing Normal University

Mary Cadenasso
University of California, Davis

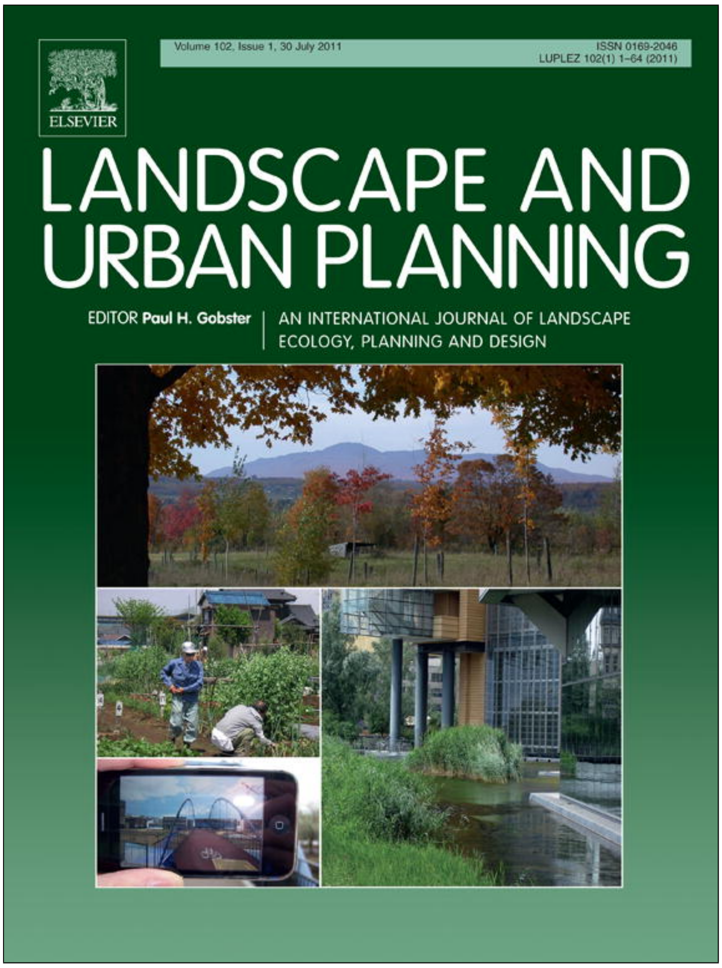
Volume 102, Issue 1, 30 July 2011
ISSN 0169-2046
LUPLEZ 102(1) 1–64 (2011)
ELSEVIER
LANDSCAPE AND URBAN PLANNING
EDITOR Paul H. Gobster
AN INTERNATIONAL JOURNAL OF LANDSCAPE ECOLOGY, PLANNING AND DESIGN

Landscape and Urban Planning 102 (2011) 54–63

Contents lists available at ScienceDirect

Landscape and Urban Planning

journal homepage: www.elsevier.com/locate/landurbplan

Does spatial configuration matter? Understanding the effects of land cover pattern on land surface temperature in urban landscapes

Weiqi Zhou [a,*], Ganlin Huang [b], Mary L. Cadenasso [a]

[a] Department of Plant Sciences, University of California, Davis, Mail Stop 1, 1210 PES, One Shields Ave, Davis, CA 95616, USA
[b] Center for Regional Change, University of California, Davis, 152 Hunt Hall, One Shields Ave, Davis, CA 95616, USA

ARTICLE INFO

Article history:
Received 15 November 2010
Received in revised form 2 March 2011
Accepted 12 March 2011
Available online 17 April 2011

Keywords:
Urban heat island
Land surface temperature
Land cover
Landscape composition and configuration
Spatial heterogeneity
Urban landscape

ABSTRACT

The effects of land cover composition on land surface temperature (LST) have been extensively documented. Few studies, however, have examined the effects of land cover configuration. This paper investigates the effects of both the composition and configuration of land cover features on LST in Baltimore, MD, USA, using correlation analyses and multiple linear regressions. Landsat ETM+ image data were used to estimate LST. The composition and configuration of land cover features were measured by a series of landscape metrics, which were calculated based on a high-resolution land cover map with an overall accuracy of 92.3%. We found that the composition of land cover features is more important in determining LST than their configuration. The land cover feature that most significantly affects the magnitude of LST is the percent cover of buildings. In contrast, percent cover of woody vegetation is the most important factor mitigating UHI effects. However, the configuration of land cover features also matters. Holding composition constant, LST can be significantly increased or decreased by different spatial arrangements of land cover features. These results suggest that the impact of urbanization on UHI can be mitigated not only by balancing the relative amounts of various land cover features, but also by optimizing their spatial configuration. This research expands our scientific understanding of the effects of land cover pattern on UHI by explicitly quantifying the effects of configuration. In addition, it may provide important insights for urban planners and natural resources managers on mitigating the impact of urban development on UHI.

1. Introduction

Approximately 50% of the world population lives in urban areas, and this proportion is projected to increase to 60% by 2030 (United Nations, 2002). In developed countries like the US, changes in urban land cover are more rapid than population growth (Alig, Kline, & Lichtenstein, 2004). The population in the US grew approximately 24% between 1980 and 2000. During roughly the same time period, however, the amount of urbanized land increased more than 34% (Alig et al., 2004). By 2025, the amount of developed land is projected to increase from 5.2% to 9.2%, or an increase of 79% (Alig et al., 2004). The changes in land use/land cover caused by urbanization greatly affect the structure and function of urban ecosystems. A well documented consequence of land conversion due to urbanization is the formation of an urban heat island (UHI) (e.g. Voogt & Oke, 2003).

Urban heat island describes the difference between urban and non-urban ambient air temperatures, which is directly related to land cover and human energy use (Oke, 1995). These differences are due to surface modifications brought about by urbanization which typically includes replacing soil and vegetation with impervious surfaces such as concrete and asphalt, and with urban structures such as buildings of various heights and densities (Akbari, Pomerantz, & Taha, 2001; Voogt & Oke, 2003). These modifications change characteristics including albedo, thermal capacity, and heat conductivity over urban areas, which in turn lead to a modified thermal climate that is warmer than surrounding non-urban areas (Voogt & Oke, 2003). Increased temperatures due to the UHI effect may increase water consumption and energy use in urban areas and lead to alterations to biotic communities (White, Nemani, Thornton, & Running, 2002). Excess heat may also affect the comfort of urban dwellers and lead to greater health risks (Poumadere, Mays, Le Mer, & Blong, 2005). In addition, higher temperatures in urban areas increase the production of ground level ozone which has direct consequences for human health (Akbari, Rosenfeld, Taha, & Gartland, 1996; Akbari et al., 2001).

Types of UHI can be loosely categorized into air temperature UHI and surface UHI (Arnfield, 2003; Nichol, Fung, Lam, & Wong,

* Corresponding author. Tel.: +1 530 754 7230; fax: +1 530 752 4361.
E-mail addresses: wqzhou@ucdavis.edu, weiqi.zhou@gmail.com (W. Zhou), glhuang@ucdavis.edu (G. Huang), mlcadenasso@ucdavis.edu (M.L. Cadenasso).

0169-2046/$ – see front matter © 2011 Elsevier B.V. All rights reserved.
doi:10.1016/j.landurbplan.2011.03.009

2009). While some studies have reported a close relationship and similar spatial patterns between surface and air temperatures (e.g. Ben-Dor & Saaroni, 1997; Nichol, 1994; Nichol et al., 2009), there is no consistent relationship between these two (Arnfield, 2003). Air temperature UHIs are generally stronger and exhibit greatest spatial variations at night, whereas the greatest difference in surface UHIs usually occurs during the daytime (Arnfield, 2003; Frey, Parlow, Vogt, Abdel Wahab, & Harhash, 2010; Nichol et al., 2009). In this study, we focus on remotely sensed land surface temperature (LST) and, consequently, surface UHI.

Remotely sensed LST records the radiative energy emitted from the ground surface, including building roofs, paved surfaces, vegetation, bare ground, and water (Arnfield, 2003; Voogt & Oke, 2003). Therefore, the pattern of land cover in urban landscapes may potentially influence LST (Arnfield, 2003; Forman, 1995). The two fundamental aspects of land cover pattern are composition and configuration (Gustafson, 1998; Turner, 2005). Composition refers to the abundance and variety of land cover features without considering their spatial character or arrangement (Gustafson, 1998; Leitao, Miller, Ahern, & McGarigal, 2006). Configuration, in contrast, refers to the spatial arrangement or distribution of land cover features. In addition to influencing LST through direct modification of surface characteristics, land cover pattern may also influence LST through its affects on the movements and flows of organisms, material, and energy in a landscape (Forman, 1995; Turner, 2005).

Previous UHI research has primarily focused on the effects of land cover composition, especially vegetation abundance, on LST (e.g. Buyantuyev & Wu, 2010; Frey, Rigo, & Parlow, 2007; Weng, Lu, & Schubring, 2004; Weng, 2009). Remotely sensed data has typically been used to evaluate LST patterns and assess the UHI, especially at vast geographic scales. Using a variety of image data, including NOAA AVHRR (Balling & Brazell, 1988), MODIS (Pu, Gong, Michishita, & Sasagawa, 2006), Landsat TM/ETM+ (Weng et al., 2004), ASTER (Lu & Weng, 2006; Pu et al., 2006) and airborne ATLAS (Lo, Quattrochi, & Luvall, 1997), these studies show that surface cover characteristics, such as vegetation abundance measured by NDVI (Normal Difference Vegetation Index), and the relative amounts of types of land use/land cover, significantly affect LST in urban areas (e.g. Buyantuyev & Wu, 2010; Liang & Weng, 2008; Weng, 2003; Weng et al., 2004; Xiao et al., 2008).

Rather than just the total amount of vegetation, the effects of the size and shape of vegetation patches on LST have been the topic of recent studies (e.g., Cao, Onishi, Chen, & Imura, 2010; Xu & Yue, 2008; Zhang, Zhong, Feng, & Wang, 2009). These studies, however, focused on vegetation patches alone, and only examined the effects of their size and shape rather than their spatial arrangement in the landscape. The relationship between landscape pattern and LST has also been investigated by examining the variations of a set of landscape metrics in different LST zones (Liu & Weng, 2009; Weng, Liu, & Lu, 2007), or in different types of land use patches (Weng, Liu, Liang, & Lu, 2008). These studies suggested that variables of landscape metrics may play an important role in the spatial patterns of LST. Few studies, however, have explored the quantitative relationship between LST and the configuration of different types of land cover features, particularly after adjusting for the effects of land cover composition.

This study investigates the effects of land cover pattern on LST in the Gwynns Falls watershed, Maryland, USA. The objectives are to: (1) examine the quantitative relationships between LST and the composition and configuration of land cover features, and (2) investigate, after adjusting for the effects of composition, whether the configuration of land cover features significantly affects LST. The results from this study can enhance our understanding of how LST varies with changing land cover patterns. In addition, important insights can be provided to urban planners and natural resource managers on how to mitigate the impact of urbanization on UHI through urban design and vegetation management.

2. Methods

2.1. Study site

This study was conducted for the Gwynns Falls watershed, the focal research watershed of the Baltimore Ecosystem Study (BES), a long-term ecological research project (LTER) of the National Science Foundation (http://www.beslter.org). The Gwynns Falls watershed, approximately 171.5 km^2 hectares in size, spans Baltimore City and Baltimore County, Maryland, USA and drains into the Chesapeake Bay (Fig. 1). It traverses an urban–suburban–rural gradient from the urban core of Baltimore City, through older inner ring suburbs to rapidly suburbanizing areas in the middle reaches and a rural/suburban fringe in the upper section. Land cover features are typical of those in urban and suburban environments, including commercial and industrial buildings, detached and multifamily houses, impervious surfaces such as concrete parking lots and sidewalks and asphalt roadways, and vegetation cover such as trees and grass. Local climate is classified as humid subtropical, with average total precipitation of 1067 mm distributed evenly throughout the year, and average monthly temperature ranging from 2 to 27 °C (UMCP, 2001).

2.2. Data

2.2.1. Measures of the composition and configuration of land cover features

Numerous metrics have been developed to measure and describe the composition and configuration of land cover features (Gustafson, 1998; McGarigal, Cushman, Neel, & Ene, 2002). For this study, we selected the most frequently used composition metric – the percent cover of each land cover feature. Configuration metrics included (Gustafson, 1998; McGarigal et al., 2002): (1) fragmentation indices: largest patch index, patch density, and edge density; (2) patch size indices: mean and standard deviation of patch size; (3) shape indices: mean and standard deviation of shape index; (4) proximity metrics: mean and standard deviation of Euclidian nearest neighbor distance; and (5) a connectivity metric: patch cohesion index, with a total of 10 metrics (Table 1). These metrics were selected because of their potential effects on LST (Forman, 1995; McGarigal et al., 2002; Turner, Gardner, & O'Neill, 2001), as well as their application in urban landscape planning (Leitao et al., 2006). The percent cover and the 10 configuration metrics were used as predictor variables in the statistical analyses to examine the relationship between LST and land cover pattern (Table 1).

The composition and configuration metrics were calculated based on a high spatial resolution land cover classification map obtained from an object-based classification approach (Zhou & Troy, 2008). Six land cover features were included in the classification map: (1) coarse-textured vegetation (CV) which includes trees and shrubs, (2) fine-textured vegetation (FV) which includes herbs and grasses, (3) bare soil, (4) pavement, (5) buildings, and (6) water (Cadenasso, Pickett, & Schwarz, 2007; Zhou & Troy, 2008). The land cover classification map was derived from aerial imagery collected for the Gwynns Falls watershed in October, 1999. The imagery has a pixel size of 0.6 m, and is 3-band color-infrared (green: 510–600 nm, red: 600–700 nm, and near-infrared: 800–900 nm). The imagery was orthorectified and meets the National Mapping Accuracy Standards for scale mapping of 1:3,000 (3-meter accuracy with 90% confidence). The overall accuracy of the classification was 92.3%, with producer's accuracies ranging from 88.3% to 100%, and user's accuracies from 83.6% to 97.7% (Zhou & Troy, 2008).

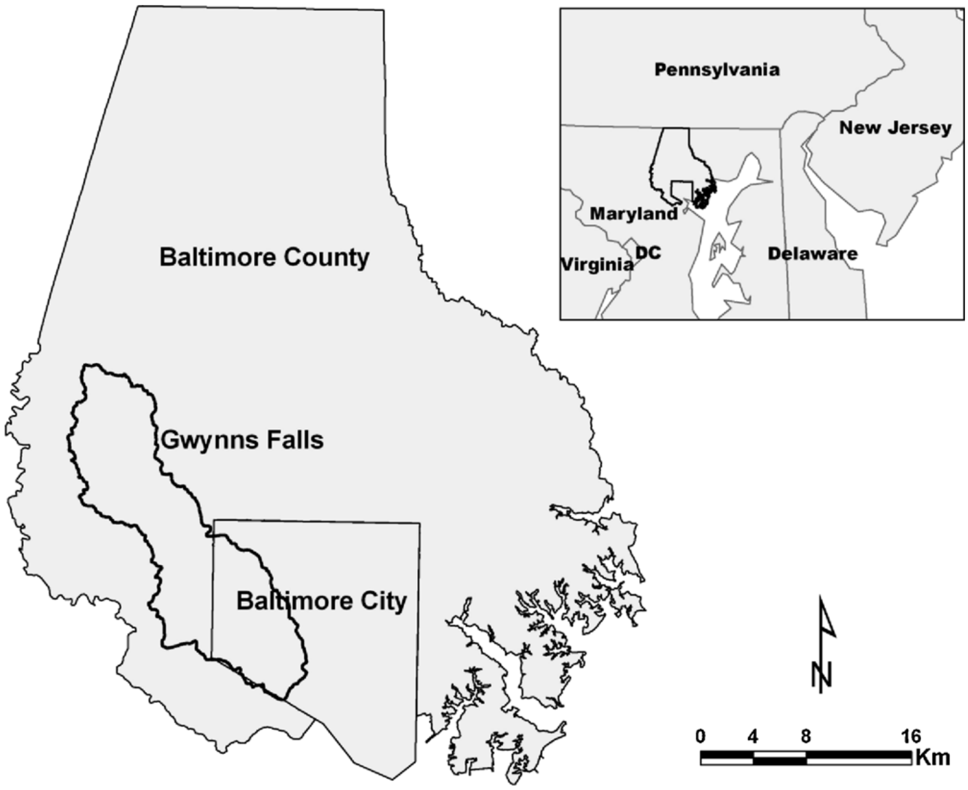

Fig. 1. The Gwynns Falls watershed includes portions of Baltimore City and Baltimore County, MD, USA, and drains into the Chesapeake Bay.

A patch layer in vector format (i.e., a polygon layer) was used to define the geographic boundaries within which to measure the composition and configuration of land cover features (Fig. 2). This patch layer was created based on a classification system called High Ecological Resolution Classification for Urban Landscapes and Environmental Systems (HERCULES). HERCULES classifies land cover and focuses on the biophysical structure of urban environments, incorporating six features of urban land heterogeneity (Cadenasso

Table 1
Description of the landscape metrics used in this study to measure the composition and configuration of land cover features within a HERCULES patch (aka McGarigal et al., 2002). These metrics were used as predictor variables. We only list the configuration variables for building as an example, but the same configuration variables were calculated for the other land cover features: pavement, coarse vegetation (CV) and fine vegetation (FV).

Variable	Description	Mean	Std.Dev.
Metrics of landscape composition (or percent cover of land cover features)			
PerBuild	Percent of buildings	0.117	0.120
PerCV	Percent of CV	0.261	0.248
PerFV	Percent of FV	0.306	0.225
PerPave	Percent of pavement	0.278	0.208
PerBS	Percent of bare soil	0.032	0.122
PerWater	Percent of water	0.007	0.065
Metrics of landscape configuration (or configuration of land cover features)			
MNPABuild	The average size of buildings within a HERCULES patch, which equals to the area occupied by buildings divided by the number of buildings.	577.15	1425.69
SDPABuild	Standard deviation of patch sizes of all building patches within a HERCULES patch; a measure of the variability of the size of buildings.	452.79	1407.93
LPIBuild	Largest patch index for building, calculated at class level, which equals to the area of the largest building within a HERCULES patch divided by the area of the HERCULES patch, multiplied by 100.	5.02	8.25
PDBuild	Patch density of buildings, the number of building patches per km^2	338.09	518.72
EDBuild	Edge density, the total length of all building patches per km^2	321.21	313.22
MNSIBuild	Mean of shape index of all building patches within a HERCULES patch; shape index is a measure of the shape complexity.	1.54	0.64
SDSIBuild	Standard deviation of shape index of all building patches within a HERCULES patch; a measure of the variability of shape complexity.	0.27	0.50
MNNNDBuild	The average distance of a building patch to its nearest neighbor building patch, calculated based on shortest edge-to-edge distance; a measure of patch isolation..	29.72	30.34
SDNNDBuild	Standard deviation of the distance of a building patch to its nearest neighbor building patch; a measure of the variability of nearest neighbor distance.	9.35	13.80
CIBuild	Patch cohesion index for building patches; a measure of connectedness of building patches.	77.76	37.88

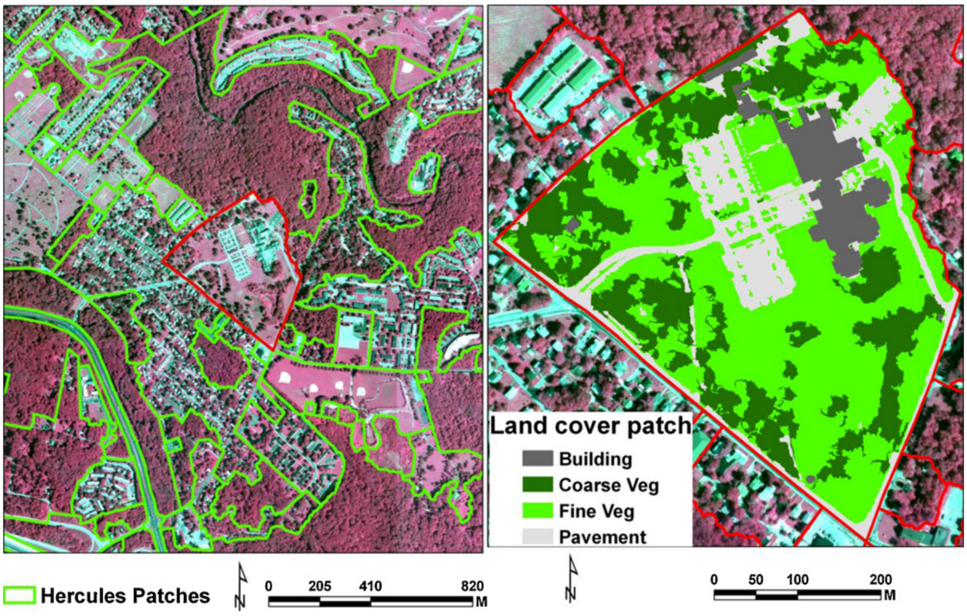

Fig. 2. HERCULES patches at different scales. Left panel: at a coarse scale (e.g., the whole watershed), HERCULES patches make up the landscape. Right panel: at a fine scale, a HERCULES patch can be viewed as a landscape itself. At this scale, the landscape is made up of patches of various land cover features (e.g., building and pavement). We focused on this finer scale and considered the HERCULES patches to be the landscapes and the different land cover features to be the patches in that landscape. The different composition and configuration of land cover features within a HERCULES patch could potentially affect land surface temperature.

et al., 2007). These six features include the first five land cover features as described above, and building type. HERCULES patches were delineated by on-screen digitizing the same imagery data used for the object-based land cover classification. The total number of patches in the watershed was 2250, with a mean patch size of about 7.6 ha (Fig. 3, panel A).

The percent cover of each of the six features, as well as the configuration metrics (McGarigal et al., 2002), were calculated in ArcGIS™ 9.3, using the HERCULES patch layer and the land cover classification map. Because we focused on the spatial distribution of specific land cover features (e.g., paved surfaces), configuration metrics were calculated at the class level. A class is a set of patches of the same type of land cover feature all within a single HERCULES patch. Metrics at the class level quantify and describe characteristics of one type of land cover feature, such as mean patch size of paved surfaces (McGarigal et al., 2002). We only calculated configuration metrics for buildings, pavement, CV and FV. We excluded bare soil and water because these two types of features had a very small proportion cover in our study site, and thus were absent from most of the HERCULES patches.

2.2.2. Land surface temperature

The LST data were derived from the thermal infrared (TIR) band (10.44–12.42 um) of a Landsat 7 Enhanced Thematic Mapper Plus (ETM+) image. The image was acquired at approximately 10:15 am local time, on July 28, 1999, a day with a highly clear atmospheric condition. As surface UHI are generally stronger and exhibit greater spatial variations during the daytime (Arnfield, 2003; Nichol et al., 2009), the selection of a daytime image in the summer is appropriate for this study. The ETM + thermal band has a spatial resolution of 60 m. The radiometric and geometrical distortions of the image were first corrected. The image was further rectified to a common Universal Transverse Mercator coordinate system based on the 1999 aerial imagery, and was resampled using the nearest neighbor algorithm with a pixel size of 60 m for the thermal band.

The digital number (DN) of the Landsat ETM + high-gain TIR band was first converted to spectral radiance (Landsat Project Science Office, 2009). The spectral radiance was then converted into at-satellite temperature (i.e., blackbody temperature) under the assumption of unity emissivity. The at-satellite temperature was corrected for varied emissivity of different land cover types, based on a map of emissivity derived from the 1999 land cover map (Lo & Quattrochi, 2003; Snyder, Wan, Zhang, & Feng, 1998). As a result, an image layer of emissivity corrected land surface temperature (unit in Kelvin) was generated (Fig. 3, panel B).

The mean LST was summarized for each HERCULES patch by overlapping the HERCULES patch boundaries and the image layer of emissivity corrected LST. The mean of LST was used as the response variable in later statistical analyses.

2.3. Statistical analyses

A Pearson correlation matrix was first developed to examine the strength of bivariate associations between LST and the variables of composition and configuration of land cover features within HERCULES patches. We further used multiple-linear regressions to examine the relationships between LST and the variables of composition and configuration. Five models were constructed and compared. The models describe LST as a function of: (1) composition variables; (2) composition variables + configuration variables for building; (3) composition variables + configuration variables for pavement; (4) composition variables + configuration variables for CV; and (5) composition variables + configuration variables for FV. The first model examines the explanatory power of the composition variables on LST, as well as their relative predictive importance. The other four models investigate whether a combination of composition variables and configuration variables for different land cover features could yield better predictions of LST. In particular, we investigated whether adding configuration variables could significantly improve the model to predict LST, after adjusting for the effects of land cover composition. The composition variables only included percent cover of building, pavement, CV, FV, and water. Bare soil was not included in the models as a composition variable because it had a non-significant correlation with LST according to the Pearson correlation analysis (Table 2).

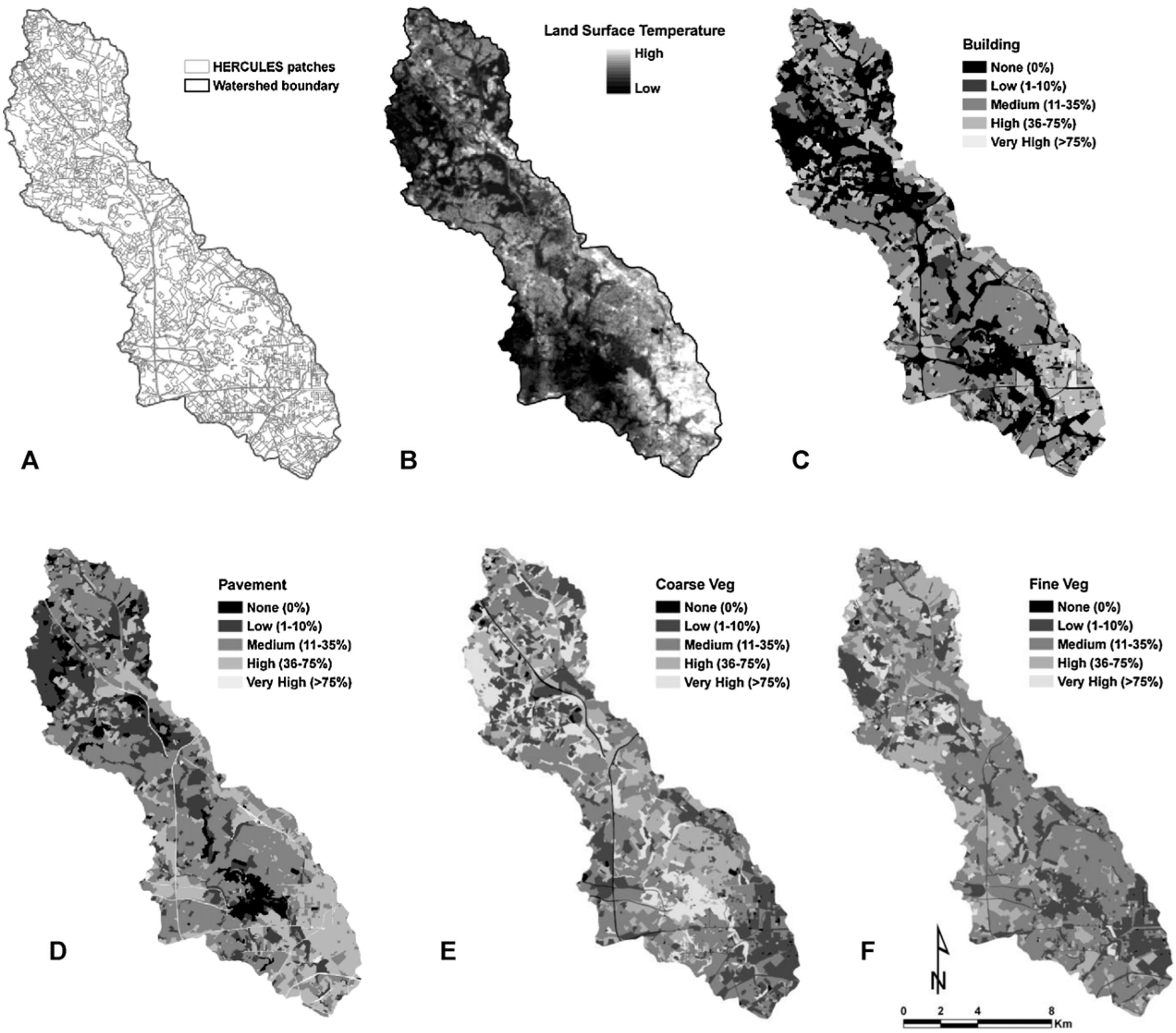

Fig. 3. The spatial pattern of land surface temperature and land cover features within the Gwynns Falls watershed. Panel A: HERCULES patches that were delineated by on-screen digitizing from high resolution imagery; Panel B: distribution of land surface temperature derived from Landsat ETM + imagery; Panel C: Percent cover of building summarized by HERCULES patches; Panel D: Percent cover of paved surfaces summarized by HERCULES patches; Panel E: Percent cover of coarse textured vegetation summarized by HERCULES patches; Panel F: Percent cover of fine textured vegetation summarized by HERCULES patches. We excluded bare soil and water as these two types of features had a very small proportion cover in our study site, and thus were absent from most of the HERCULES patches.

Table 2
Pearson correlation coefficients between LST and variables of composition and configuration of land cover features. For example, the cell value of 0.41, as highlighted, is the correlation coefficient between LST and the largest patch index of building. We only included the configuration variables for building, pavement, CV and FV in this study.

		Land cover features					
		Building	Pave	CV	FV	Bare soil	Water
Composition	Percent cover	0.57**	0.55**	−0.47**	−0.25**	−0.02	−0.10**
Configuration	Largest patch index	**0.41****	0.55**	−0.45**	−0.22**		
	Patch density	0.16**	0.04	0.31**	0.20**		
	Edge density	0.42**	0.49**	−0.30**	−0.18**		
	Mean patch size	0.20**	0.17**	−0.24**	−0.10**		
	Standard deviation of patch size	0.18**	0.14**	−0.22**	−0.16**		
	Mean shape index	0.14**	0.16**	−0.30**	−0.22**		
	Standard. deviation of shape index	0.14**	0.16**	−0.34**	−0.24**		
	Mean nearest neighbor distance	0.07**	0.09**	−0.32**	−0.13**		
	Standard deviation of nearest neighbor distance	0.05*	−0.12**	−0.26**	−0.17**		
	Cohesion index	0.24**	0.17**	−0.14**	−0.17**		

* Correlation is significant at the 0.05 level (two-tailed).
** Correlation is significant at the 0.01 level (two-tailed).

3. Results

3.1. Effects of the composition of land cover features on LST

The Pearson correlation coefficients show that all of the composition variables, except bare soil, were significantly related to LST (Table 2), with some variables having stronger relationships with LST than others. Composition variables such as percent cover of buildings, pavement and CV had relatively strong relationships with LST, while percent cover of FV and water were only weakly related to LST. Fig. 3 shows that locations with high LST (panel B) generally have high percent cover of buildings (panel C) and paved surfaces (panel D), but low percent cover of CV (panel E) and FV (panel F). Locations with low LST, in contrast, have low percent cover of building and paved surfaces, but high percent cover of vegetation.

Approximately 43.4% of the variation in LST was explained jointly by the five composition variables. Among the five types of land cover features, percent cover of building (*PerBuild*) was the most significant variable in predicting LST, followed by the percent cover of CV (*PerCV*) (Model 1, Table 3). All variables were significant at the 99% confidence level, except for percent cover of FV (*PerFV*), which was significant at the 95% confidence level. A positive coefficient for an independent variable indicates that the variable has a positive effective on LST, or that LST increases with the increase of the value of that variable; whereas a negative coefficient indicates LST decreases with the increase of the value of that variable. For example, both coefficients of percent cover of building and pavement (*PerPave*) were positive, suggesting that an increase in the percent cover of building and pavement would increase LST (Model 1, Table 3). In contrast, the negative coefficients of percent cover of CV, FV and water (*PerWater*) indicated that LST would decrease with the increase of relative abundances of vegetation and water (Model 1, Table 3).

3.2. Effects of the configuration of land cover features on LST

The Pearson correlation analysis showed that some of the configuration variables had as strong a bivariate relationship with LST as that of their corresponding composition variables (Table 2). For example, the correlation coefficient of edge density of pavement was close to that of percent cover of pavement, and the correlation between LST and the largest patch index of pavement was as strong as that of percent cover of pavement with LST. In most cases, however, the Pearson correlation coefficients of configuration variables were smaller than those of their corresponding composition variables (Table 2).

Although results from the multiple-linear regressions indicated that variables of land cover configuration are important predictors of LST, a combination of composition and configuration variables better predicts the variation. Many of the configuration variables could significantly add to the explanation of LST, even after adjusting for the effects of land cover composition. Below, we present the results of the effects of the configuration variables of each land cover feature on LST.

Building: All of the variables describing the configuration of buildings were significantly correlated to LST in the bivariate correlation analysis (Table 2). Largest patch index (*LPIBuild*) and building edge density (*EDBuild*) had a relatively strong relationship with LST, whereas the mean (*MNNNDBuild*) and standard deviation (*SDNNDBuild*) of nearest neighbor distance among buildings were weakly related to LST. Approximately 45.5% of the variation in LST was explained jointly by the five composition variables and building configuration variables (Model 2, Table 3).

After adjusting for the effects of the landscape composition variables, largest patch index, patch density (*PDBuild*), edge density, mean (*MNSIBuild*) and standard deviation (*SDSIBuild*) of shape index, and mean of nearest neighbor distance remained significantly associated with LST, whereas the other variables lost significance ($P < 0.05$) (Model 2, Table 3). Among those configuration variables, building edge density was the most important one. When taking into account the effects of building configuration, percent cover of FV lost significance. Edge density, large patch index, and mean of nearest neighbor distance had a negative effect on LST, suggesting LST decreases with the increase of building edge density, largest patch index and nearest neighbor distances among buildings. Patch density, mean and standard deviation of shape index, however, had a positive effect on LST, indicating that LST increases with the increase of building patch density, and shape complexity and variability of buildings.

Pavement: All pavement configuration variables were significantly correlated with LST in the bivariate correlation analysis, except for patch density (Table 2). Largest patch index (*LPIPave*) and edge density (*EDPave*) were relatively strongly correlated with LST. A combination of the five composition variables and pavement configuration variables explained about 45.7% of the variation in LST (Model 3, Table 3).

After adjusting for the effects of composition, largest patch index, mean (*MNSIPave*) and standard deviation (*SDSIPave*) of shape index, and standard deviation of nearest neighbor distance (*SDNNDPave*) remained significant (Model 3, Table 3). Among those configuration variables, largest patch index was the most important one. Interestingly, patch density (*PDPave*) became significant when adjusting for the effects of other composition and configuration variables. In addition, percent cover of pavement (*PerPave*) was no longer significant when adding the configuration variables of pavement. This might be due to the fact that the percent cover of pavement was highly correlated to largest patch index ($r = 0.976$).

The positive coefficient of largest patch index and the negative coefficient of patch density indicated that LST increases when the paved surfaces are less fragmented, holding land cover composition constant. In addition, LST increases with the increase of shape complexity and variability of paved patches. LST, however, decreases with the increased variability of nearest neighbor distances among paved surfaces.

CV: All the CV configuration variables were significantly correlated with LST in the bivariate correlation analysis, among which the largest patch index was the most significant one (Table 2). Approximately 47.1% of variation in LST was explained jointly by the five composition variables and CV configuration variables (Model 4, Table 3).

Five configuration variables remained significantly related to LST after adjusting for the effects of the composition variables (Model 4, Table 3). These included edge density (*EDCV*), standard deviation of shape index (*SDSICV*), mean (*MNNNDCV*) and standard deviation (*SDNNDCV*) of nearest neighbor distance, and cohesion index (*CICV*). Among these configuration variables, mean of nearest neighbor distance and edge density were the most important. Edge density, mean and standard deviation of nearest neighbor distance, and standard deviation of shape index had a negative effect on LST, suggesting LST decreases with the increase of CV edge density, nearest neighbor distance and its variability among CV, and variability of shape complexity. LST, however, increases with the increased degree of CV connectivity.

FV: All of the configuration variables of FV were significantly, but weakly, correlated to LST in the bivariate correlation analysis (Table 2). Approximately 45.5% of variation in LST was explained jointly by the five composition variables and FV configuration variables (Model 5, Table 3). Four variables, edge density (*EDFV*), standard deviation of patch size (*SDPAFV*), mean of shape index (*MNSIFV*), and cohesion index (*CIFV*) remained significant after adjusting for the effects of composition on LST. Edge density was

Table 3

Summary results for the five multi-linear regression models. For each of the five models, the response variable, LST, was predicted by composition variables, i.e., percent cover of five land cover features (model 1), or a combination of those composition variables with the configuration variables of one type of land cover feature. The shaded columns for Model 2–5 are the composition variables.

Model	Explanatory variables/regression coefficient; standardized coefficient R-square (adjusted)[a]															
	PerBuild	PerPave	PerCV	PerFV	PerWater											
Model 1	.73** (0.33)	3.41** (0.20)	−3.43** (−0.24)	−1.03* (−0.07)	−3.73** (−0.07)											0.434 (0.432)
	PerBuild	PerPave	PerCV	PerFV	PerWater	LPI-Build	PD-Build	ED-Build	MNPA-Build	SDPA-Build	MNSI-Build	SDSI-Build	MNNND-Build	SDNND-Build	CIBuild	
Model 2	18.47** (0.63)	3.62** (0.21)	−3.20** (−0.23)	−0.74 (−0.05)	−4.23** (−0.08)	−0.034** (−0.08)	3.4E−4* (0.05)	−0.003** (−0.26)	−9.71E−5 (−0.04)	−5.81E−5 (−0.02)	0.32** (0.06)	0.48** (0.07)	−0.008** (−0.07)	−0.003 (−0.01)	−0.004 (−0.04)	0.455 (0.452)
	Per-Build	Per-Pave	PerCV	PerFV	Per-Wsater	LPI-Pave	PD-Pave	ED-Pave	MNPA-Pave	SDPA-Pave	MNSI-Pave	SDSI-Pave	MNNND-Pave	SDNND-Pave	CI-Pave	
Model 3	9.75** (0.33)	−2.29 (−0.14)	−3.79** (−0.27)	−1.34** (−0.09)	−4.43** (−0.08)	0.047** (0.29)	−4.82E−4* (−0.07)	2.78E−4 (0.04)	−1.27E−5 (−0.02)	−1.61E−5 (−0.04)	0.32** (0.07)	0.29** (0.06)	0.001 (0.00)	−0.015* (−0.04)	−0.006 (−0.01)	0.457 (0.453)
	Per-Build	Per-Pave	PerCV	PerFV	Per-Water	LPICV	PDCV	EDCV	MNP-ACV	SDP-ACV	MNS-ICV	SDS-ICV	MNNN-DCV	SDNN-DCV	CICV	
Model 4	8.76** (0.30)	2.46** (0.15)	−2.36* (−0.17)	−0.84 (−0.05)	−4.31** (−0.08)	0.002 (0.02)	−8.76E−6 (−0.01)	−0.001** (−0.13)	1.87E−6 (0.01)	−8.43E−6 (−0.04)	0.027 (0.01)	−0.578** (−0.11)	−0.031** (−0.14)	−0.017* (−0.05)	0.017** (0.05)	0.471 (0.467)
	Per-Build	Per-Pave	PerCV	PerFV	Per-Water	LPIFV	PDFV	EDFV	MNPA-FV	SDPA-FV	MNSI-FV	SDSI-FV	MNNND-FV	SDNND-FV	CIFV	
Model 5	9.34** (0.32)	3.50** (0.21)	−3.26** (−0.23)	1.55 (0.10)	−2.27* (−0.04)	−0.006 (−0.04)	1.35E−4 (0.03)	−0.001** (−0.17)	−6.28E−6 (−0.01)	−5.62E−5** (−0.07)	−0.53** (−0.06)	−0.085 (−0.01)	−0.001 (−0.00)	−0.024 (−0.04)	0.022** (0.04)	0.455 (0.451)

[a] We included both the unstandardized regression coefficients and standardized coefficients (included in the parentheses). The standardized coefficients (beta coefficients, or beta weights) are used to determine the relative importance of explanatory variables. The larger the absolute value of the standardized coefficient, the more important a variable.

* Coefficient is significant at the 0.05 level (two-tailed).

** Coefficient is significant at the 0.01 level (two-tailed).

the most important configuration variable. When considering the effects of FV configuration on LST, the percent cover of FV (*PerFV*) was no longer significant. Edge density, standard deviation of patch size, and mean of shape index had a negative effect on LST, indicating that LST decreases with the increase of FV edge density, variability of patch size, and shape complexity; whereas LST increases with the increase of FV cohesion index.

4. Discussion

Our results indicated that both the composition and configuration of land cover features significantly affects the magnitude of LST. By explicitly describing the quantitative relationships of LST with the composition and configuration of land cover features; this research expands our scientific understanding of the effects of land cover pattern on LST in urban landscapes. These results have important theoretical and management implications. Urban planners and natural resource managers attempting to mitigate the impact of urban development on UHI can gain insights into the importance of balancing the relative amount of various types of land cover features and optimizing their spatial distributions.

4.1. Theoretical implications

The effects of land cover composition on LST have been extensively documented (e.g., Buyantuyev & Wu, 2010; Liang & Weng, 2008; Weng, 2009; Xiao et al., 2008). Our results are consistent with those from previous research that land cover composition, or the percent cover of different types of land cover features, greatly affect the magnitude of LST. In fact, our results showed that the composition of land cover features is a more important factor in determining LST than the configuration of those features. Increasing vegetation cover or surface water could significantly decrease LST, and thus help to mitigate excess heat in urban areas; whereas the increase of buildings and paved surfaces would significantly increase LST, exacerbating the UHI phenomena.

The land cover feature that most significantly affects the magnitude of LST is the percent cover of buildings. In contrast, percent cover of woody vegetation is the most important factor mitigating UHI effects. These results may be due to the fact that changes in percent cover of buildings and woody vegetation lead to modifications of the land surface characteristics such as albedo and evapotranspiration. In addition, an increase in building cover is also associated with the production of waste heat from air conditioning and refrigeration systems, as well from motorized vehicular traffic – all of which exacerbates the UHI effects. These results suggest that the UHI effect can be effectively mitigated by using light-colored materials on houses and roofs, implementing green roofs, and increasing the amount of tree canopies. Water bodies had a weak relationship with LST, and bare soil was not significantly correlated to LST. This may be partly due to the very small proportion cover of these two types of features in our study area.

The configuration of land cover features also significantly affects LST. For a fixed relative amount of land cover features, LST can be significantly increased or decreased by different spatial arrangements of those features. This is because the spatial arrangement influences the flow of energy, or energy exchange among land cover features (Forman, 1995) and, thus, affects LST.

The configuration of all four land cover features – buildings, pavement, CV and FV – significantly affects the magnitude of LST. The significance and effect of specific configuration variables on LST, however, varied broadly among the land cover features. For example, edge density is a very important configuration variable that affects LST. Given a fixed composition of land cover features, an increase in edge density of woody and herbaceous vegetation significantly decreases the magnitude of LST. In addition, LST generally decreases with the increase of shape complexity and variability of woody and herbaceous vegetation. Increase in edge density and shape complexity of woody vegetation may increase shade, provided by woody vegetation, for surrounding areas and thus, reduce LST. In addition, higher edge density and increased shape complexity of woody and herbaceous vegetation may enhance the interactions between vegetation and built-up areas (building & paved surfaces), and thus facilitate energy exchange among land cover features, resulting in a lower mean LST (Forman, 1995; Xu & Yue, 2008). Land surface temperature is also predicted to decrease with an increase of the average and variability of nearest neighbor distance among woody vegetation. This suggests that an evenly distributed, rather than clustered, pattern of woody vegetation can further reduce LST. This may be because, given a fixed percent cover of woody vegetation, an even distribution can provide more shade for surrounding non-woody vegetated areas and enhance the interactions between woody vegetation and other land cover features than had the woody vegetation been clustered. This was further supported by the effect of the cohesion index which indicated that an increase in the degree of woody vegetation connectivity would increase LST because, as patch cohesion increases, the woody vegetation becomes more clumped or aggregated in its distribution (McGarigal et al., 2002).

The effects of the configuration of building and paved surfaces on LST appear more complicated. Land surface temperature decreases with the increase of building largest patch index, mean distances among buildings, and patch density of paved surfaces. Land surface temperature, however, increases with the increase of largest patch index of paved surfaces, and patch density of buildings. In contrast to vegetation, an increase in shape complexity and variability of buildings and paved surfaces leads to an increase in LST. This result reveals the complex thermal environments characteristic of urban landscapes. On the one hand, the increase in shape complexity and variability of buildings and paved surfaces may facilitate energy exchange between built-up areas and vegetation, and thus cool the built-up areas (Forman, 1995; Xu & Yue, 2008; Zhang et al., 2009). On the other hand, the increase in shape complexity and variability of buildings and paved surfaces may increase solar heat gain to buildings and paved surfaces because of the increased exposed surfaces (Voogt & Oke, 1998).

Our results also highlighted that, when testing the effects of configuration of land cover features on LST, it is important to control for the effects of their composition. This is because configuration metrics are commonly correlated with composition metrics (McGarigal et al., 2002; Riitters et al., 1995), resulting in spurious correlations between LST and some configuration variables in bivariate analyses. The surprising result that the mean patch size of land cover features was not significantly correlated to LST for any feature type after adjusting for the effects of composition may be due to the mean patch size and composition variables being strongly correlated (McGarigal et al., 2002; Riitters et al., 1995). Our results showed that all configuration variables of the four land cover features were significantly correlated to LST in the bivariate analysis. Fewer of these variables, however, remained significant after adjusting for the effects of land cover composition. Similar results were also found in Weng et al. (2008), when using factor analysis.

The combination of composition and configuration of land cover features only explained about half of the variance in LST. This is lower than reported by some previous studies (e.g. Buyantuyev & Wu, 2010; Liang & Weng, 2008). The research presented here, however, was conducted at a finer scale (a smaller area of unit of analysis) than those previous studies. In general, a stronger correlation between LST and land cover variables can be found at coarser scales. Thus, a greater proportion of the variance in LST can be explained by land cover variables at the coarser scale (Liang & Weng, 2008). This may suggest that, at a fine scale, more factors should be considered to better predict LST than land cover pattern. This may be due to the fine-scale complexity of the urban thermal environments (Arnfield, 2003). For example, the impacts of the three dimensional structure of urban surfaces at the fine-scale, such as building and tree height and ruggedness of the urban surface, should be included to improve the prediction of the models (Arnfield, 2003; Voogt & Oke, 1998; Voogt & Oke, 2003).

4.2. Management implications

There is an increasing interest in linking the emerging theory of urban ecology to ecological design and management of urban landscapes (McGrath et al., 2007; Cadenasso & Pickett, 2008; Pickett & Cadenasso, 2008). The results that both the composition and configuration of land cover features in a landscape significantly affected the magnitude of LST can provide important insights into ecological design and management, and, therefore, may have important implications for urban planners and natural resource managers. This suggests that the impact of urbanization on the UHI can be mitigated by balancing the relative amounts of various land cover features and optimizing their spatial configuration.

Vegetation management, particularly increasing tree canopy, has been considered an effective means to mitigate excess urban heat. For highly urbanized areas, while removal of paved surfaces or buildings maybe expensive and impractical (Kaiser, Godschalk, & Stuart, 1995), the amount and spatial distribution of vegetation can be altered through vegetation management such as tree planting in selected locations. Many US cities, such as Baltimore and New York, have established goals to increase tree canopy cover in order to enhance ecosystem services and reduce the impact of urban development on, for example, heat island effects, water consumption and stormwater runoff (Maryland Department of Natural Resources, 2007). Previous research has focused on where trees could potentially be planted (Troy, Grove, O'Neil-Dunne, Pickett, & Cadenasso, 2007; Wu, Xiao, & McPherson, 2008). Results from this study can provide additional insights for urban planners and natural resources managers about how to arrange those trees so that the spatial configuration of the tree canopy can be optimized to maximize the canopy's mitigating affects on the UHI.

The configuration of land cover features other than trees also significantly affects LST. This result has important implications for urban design and planning, particularly for locations where urbanization is still in process. It suggests that by designing landscapes that balance the relative amounts of various land cover features and that optimize their spatial configuration, the impact of urbanization on LST can be greatly mitigated.

4.3. Limitations

This study has its limitations. The research was conducted for one region, using only one daytime thermal image to obtain LST. Previous studies have shown that there are diurnal and seasonal variations in the relationships between LST and land cover features (e.g. Buyantuyev & Wu, 2010; Yuan & Bauer, 2007). For example, vegetation abundance, measured by NDVI, had a strong relationship with daytime LST, but was only very weakly related to nighttime LST (Buyantuyev & Wu, 2010). The relationship between LST and vegetation abundance also varies by seasons (Yuan & Bauer, 2007). In addition, different climatic conditions may significantly influence the amplitude of daytime surface UHI (Imhoff, Zhang, Wolfe, & Bounoua, 2010). Therefore, further studies that use multiple daytime and nighttime thermal images for different seasons are desirable. In addition, comparison studies across metropolitan areas under different climatic conditions are recommended.

5. Summary and conclusions

Urban heat island is a critical consequence of urbanization due to land cover conversions. Understanding the link between land cover patterns and UHI is important for designing effective mechanisms to mitigate the impact of urbanization on UHI. This study investigates the quantitative relationships of LST with both the composition and configuration of land cover features in urban landscapes. The results indicated that not only does the composition of land cover features significantly affect the magnitude of LST, but so does the configuration of those features. However, the composition of land cover features is more important in determining LST than their configuration. The land cover feature that most significantly affects the magnitude of LST is the percent cover of buildings. In contrast, percent cover of woody vegetation is the most important factor mitigating UHI effects. These results suggest that the UHI effect can be effectively mitigated by using light-colored materials on houses and roofs, implementing green roofs, and increasing the amount of tree canopies. The configuration of land cover features also matters. Holding composition constant, LST can be significantly increased or decreased by different spatial arrangements of land cover features. For example, an increase in edge density, and shape complexity and variability of woody and herbaceous vegetation significantly decreases the magnitude of LST. In contrast, an increase in shape complexity and variability of buildings and paved surfaces leads to an increase in LST. In addition, an increase of the average and variability of nearest neighbor distance among woody vegetation can significantly decrease LST. Similarly, an increase of the average nearest neighbor distance among buildings can also significantly decrease LST. Therefore, the impact of urbanization on UHI can be mitigated not only by balancing the relative amounts of various land cover features, but also by optimizing their spatial configuration. This finding provides important insights for urban planners and natural resource managers on urban heat mitigation through urban design and vegetation management, for both highly urbanized areas and areas where urbanization is still in process. While we found spatial configuration of land cover features does matter, it should be noted that this conclusion is based on LST data from one daytime thermal image, and the research was conducted only for one metropolitan area. Whether this conclusion can be applied to different seasons and other metropolitan areas should be further explored. Therefore, future comparison studies across metropolitan areas under different climatic conditions, and studies that use multiple daytime and nighttime thermal images for different seasons are recommended.

References

Akbari, H., Rosenfeld, A., Taha, H., & Gartland, L. (1996). Mitigation of summer urban heat islands to save electricity and smog. In *76th Annual American Meteorological Society Meeting* Atlanta, GA,

Akbari, H., Pomerantz, M., & Taha, H. (2001). Cool surfaces and shade trees to reduce energy use and improve air quality in urban areas. *Solar Energy*, *70*, 295–310.

Alig, R. J., Kline, J. D., & Lichtenstein, M. (2004). Urbanization on the US landscape: Looking ahead in the 21st century. *Landscape and Urban Planning*, *69*, 219–234.

Arnfield, A. J. (2003). Two decades of urban climate research: A review of turbulence, exchanges of energy and water, and the urban heat island. *International Journal of Climatology*, *23*, 1–26.

Balling, R. C., & Brazell, S. W. (1988). High resolution surface temperature pattern in a complex urban terrain. *Photogrammetric Engineering and Remote Sensing*, *54*, 1289–1293.

Ben-Dor, E., & Saaroni, H. (1997). Airborne video thermal radiometry as a tool for monitoring microscale structures of the urban heat island. *International Journal of Remote Sensing*, *18*(4), 3039–3053.

Buyantuyev, A., & Wu, J. (2010). Urban heat islands and landscape heterogeneity: Linking spatiotemporal variations in surface temperatures to land-cover and socioeconomic patterns. *Landscape Ecology*, *25*(1), 17–33.

Cadenasso, M. L., Pickett, S. T. A., & Schwarz, K. (2007). Spatial heterogeneity in urban ecosystems: Reconceptualizing land cover and a framework for classification. *Frontier in Ecological Environment*, *5*, 80–88.

Cadenasso, M. L., & Pickett, S. T. A. (2008). Urban principles for ecological landscape design and maintenance: Scientific fundamentals. *Cities and the Environment*, *1*(2), 1–16.
Cao, X., Onishi, A., Chen, J., & Imura, H. (2010). Quantifying the cool island intensity of urban parks using ASTER and IKONOS data. *Landscape and Urban Planning*, *96*(4), 224–231.
Forman, R. T. T. (1995). *Land mosaics: The ecology of landscape and regions*. NY: Cambridge University Press.
Frey, C. M., Rigo, G., & Parlow, E. (2007). Urban radiation balance of two coastal cities in a hot and dry environment. *International Journal of Remote Sensing*, *28*(12), 2695–2712.
Frey, C. M., Parlow, E., Vogt, R., Abdel Wahab, M., & Harhash, M. (2010). Flux measurements in Cairo. Part 1. In situ measurements and their applicability for comparison with satellite data. *International Journal of Climatology*, *31*, 218–231.
Gustafson, E. J. (1998). Quantifying landscape spatial pattern: What is the state of the art? *Ecosystems*, *1*, 143–156.
Imhoff, M. L., Zhang, P., Wolfe, R. E., & Bounoua, L. (2010). Remote sensing of the urban heat island effect across biomes in the continental USA. *Remote Sensing of Environment*, *114*(3), 504–513.
Kaiser, E. J., Godschalk, D. R., & Stuart, C. F. (1995). *Urban land use planning*. Chicago: University of Illinois Press.
Landsat Project Science Office, 2009. Landsat 7 Science Data User's Handbook. URL: http://landsathandbook.gsfc.nasa.gov/handbook.html, Goddard Space Flight Center, NASA, Washington, DC (last date accessed: 16 August 2010).
Leitao, A. B., Miller, J., Ahern, J., & McGarigal, K. (2006). *Measuring landscapes: A planner's handbook*. Washington, DC: Island Press.
Liang, B., & Weng, Q. (2008). Multi-scale analysis of census-based land surface temperature variations and determinants in Indianapolis, United States. *Journal of Urban Planning D-ASCE*, *134*(3), 129–139.
Liu, H., & Weng, Q. (2009). Scaling-up effect on the relationship between landscape pattern and land surface temperature. *Photogrammetric Engineering and Remote Sensing*, *75*(3), 291–304.
Lo, C. P., Quattrochi, D. A., & Luvall, J. C. (1997). Application of high-resolution thermal infrared remote sensing and GIS to assess the urban heat island effect. *International Journal of Remote Sensing*, *18*, 287–304.
Lo, C. P., & Quattrochi, D. A. (2003). Land-use and land-cover change, urban heat island phenomenon, and health implications: A remote sensing approach. *Photogrammetric Engineering and Remote Sensing*, *69*, 1053–1063.
Lu, D., & Weng, Q. (2006). Spectral Mixture Analysis of ASTER Images for Examining the Relationship between Urban Thermal Features and Biophysical Descriptors in Indianapolis, United States. *Remote Sensing of Environment*, *104*(2), 157–167.
Maryland Department of Natural Resources, 2007. Chesapeake Bay urban tree canopy goals, http://www.dnr.state.md.us/forests/programs/urban/urbantreecanopygoals.asp (Accessed on October 14, 2009).
McGarigal, K., Cushman, S. A., Neel M. C., & Ene, E. (2002). FRAGSTATS: Spatial Pattern Analysis Program for Categorical Maps. Computer software program produced by the authors at the University of Massachusetts, Amherst. Available at the following web site: http://www.umass.edu/landeco/research/fragstats/fragstats.html.
McGrath, B. P., Marshall, V., Cadenasso, M. L., Grove, J. M., Pickett, S. T. A., & Plunz, R., et al. (2007). Designing Patch Dynamics. Columbia Graduate School of Architecture, Planning and Preservation. New York.
Nichol, J. E. (1994). A GIS-based approach to microclimate monitoring in Singapore's high-rise housing estates. *Photogrammetric Engineering and Remote Sensing*, *60*, 1225–1232.
Nichol, J. E., Fung, W. Y., Lam, K., & Wong, M. S. (2009). Urban heat island diagnosis using ASTER satellite images and 'in situ' air temperature. *Atmospheric Research*, *94*(2), 276–284.
Oke, T. R. (1995). The heat island of the urban boundary layer: Characteristics, causes and effects. In J. E. Cermak (Ed.), *Wind climate in cities* (pp. 81–107). Netherlands: Kluwer Academic Publishers.
Pickett, S. T. A., & Cadenasso, M. L. (2008). Linking ecological and built components of urban mosaics: An open cycle of ecological design. *Journal of Ecology*, *96*, 8–12.
Poumadere, M., Mays, C., Le Mer, S., & Blong, R. (2005). The 2003 heat wave in France: Dangerous climate change here and now. *Risk Annual*, *25*(6), 1483–1494.
Pu, R., Gong, P., Michishita, R., & Sasagawa, T. (2006). Assessment of multi-resolution and multi-sensor data for urban surface temperature retrieval. *Remote Sensing of Environment*, *104*, 211–225.
Riitters, K. H., O'Neill, R. V., Hunsaker, C. T., Wickham, J. D., Yankee, D. H., Timmins, S. P., et al. (1995). A factor analysis of landscape pattern and structure metrics. *Landscape Ecology*, *10*, 23–39.
Snyder, W. C., Wan, Z., Zhang, Y., & Feng, Y. Z. (1998). Classification-based emissivity for land surface temperature measurement from space. *International Journal of Remote Sensing*, *19*(14), 2753–2774.
Troy, A. R., Grove, J. M., O'Neil-Dunne, J. P. M., Pickett, S. T. A., & Cadenasso, M. L. (2007). Predicting patterns of vegetation and opportunities for greening on private urban lands. *Environmental Management*, *40*, 394–412.
Turner, M. G., Gardner, R. H., & O'Neill, R. V. (2001). *Landscape ecology in theory and practice*. New York: Springer-Verlag.
Turner, M. G. (2005). Landscape ecology: What is the state of the science? *Annual Review of Ecological Evolution and Sensing*, *36*, 319–344.
United Nations. (2002). *World urbanization prospects – the 2001 revision data table and highlights*. New York: Department of Economic and Social Affairs.
University of Maryland, College Park, 2001. Normal Precipitation and Temperature Values for Baltimore City from 1961 to 1990. Baltimore, Maryland.
Voogt, J. A., & Oke, T. R. (1998). Effects of urban surface geometry on remotely-sensed surface temperature. *International Journal of Remote Sensing*, *19*, 895–920.
Voogt, J. A., & Oke, T. R. (2003). Thermal remote sensing of urban climates. *Remote Sensing of Environment*, *86*, 370–384.
Weng, Q. (2003). Fractal analysis of satellite-detected urban heat island effect. *Photogrammetric Engineering and Remote Sensing*, *69*(5), 555–566.
Weng, Q., Liu, H., & Lu, D. (2007). Assessing the effects of land use and land cover patterns on thermal conditions using landscape metrics in city of Indianapolis, United States. *Urban Ecosystem*, *10*(2), 203–219.
Weng, Q., Liu, H., Liang, B., & Lu, D. (2008). The spatial variations of urban land surface temperatures: Pertinent factors, zoning effect, and seasonal variability. *IEEE Journal of Selected Topics in Applied Earth Observations & Remote Sensing*, *1*(2), 154–166.
Weng, Q., Lu, D., & Schubring, J. (2004). Estimation of land surface temperature – vegetation abundance relationship for urban heat island studies. *Remote Sensing of Environment*, *89*, 467–483.
Weng, Q. (2009). Thermal infrared remote sensing for urban climate and environmental studies: Methods, applications, and trends. *ISPRS Journal of Photogrammetry and Remote Sensing*, *64*, 335–344.
White, M. A., Nemani, R. R., Thornton, P. E., & Running, S. W. (2002). Satellite evidence of phenological differences between urbanized and rural areas of the eastern United States deciduous broadleaf forest. *Ecosystems*, *5*, 260–277.
Wu, C., Xiao, Q., & McPherson, E. G. (2008). A method for locating potential tree-planting sites in urban areas: A case study of Los Angeles, USA. *Urban Forestry and Urban Green*, *7*(2), 65–76.
Xiao, R., Weng, Q., Ouyang, Z., Li, W., Schienke, E., & Zhang, Z. (2008). Land surface temperature variation and major factors in Beijing, China. *Photogrammetric Engineering and Remote Sensing*, *74*(4), 451–461.
Xu, L., & Yue, W. (2008). A study on thermal environment effect of urban park landscape. *Acta Ecologica Sinica*, *28*(4), 1702–1710.
Yuan, F., & Bauer, M. E. (2007). Comparison of impervious surface area and normalized difference vegetation index as indicators of surface urban heat island effects in Landsat imagery. *Remote Sensing of Environment*, *106*, 375–386.
Zhang, X., Zhong, T., Feng, X., & Wang, K. (2009). Estimation of the relationship between vegetation patches and urban land surface temperature with remote sensing. *International Journal of Remote Sensing*, *30*(8), 2105–2118.
Zhou, W., & Troy, A. (2008). An object-oriented approach for analyzing and characterizing urban landscape at the parcel level. *International Journal of Remote Sensing*, *29*(11), 3119–3135.